Sarcoidosis Manifesting as a Pseudotumorous Renal Mass

Scott Goldsmith[1], Matt Harris[1], Kurt Scherer[1], Samer Al-Quran[2], Elizabeth Vorhis[1*]

1. Department of Radiology, University of Florida College of Medicine, Gainesville, Florida, USA

2. Department of Pathology, University of Florida College of Medicine, Gainesville, Florida, USA

* **Correspondence:** Elizabeth Vorhis, University of Florida COM, Department of Radiology, 1600 Archer Road, Box 100374, Gainesville, FL 32610-0374, USA
(*srgoldsmith@ufl.edu*)

Radiology Case. 2013 May; 7(5):23-34 :: DOI: 10.3941/jrcr.v7i5.1316

ABSTRACT

A 53 year-old African American woman with a three-year history of pulmonary sarcoidosis had a follow-up computed tomographic scan to evaluate the status of her disease and response to treatment. On the scan, an abnormal, hypodense mass on the left renal superior pole, which was not present on previous scans, was incidentally discovered. The initial concern was of carcinoma, despite her lack of any urinary symptoms. She underwent further evaluation with magnetic resonance, and the enhancement pattern and the shape of the mass were more suggestive of lymphoma or infarction than a carcinoma. A review of literature revealed sparse case reports demonstrating sarcoidosis presenting as infiltrative granulomatous masses resembling tumors with nonspecific imaging qualities. This diagnosis was entertained and then proven by biopsy. Pseudotumorous renal sarcoid should be in the differential of renal masses, especially in patients with a history of sarcoidosis, as it alters clinical management.

CASE REPORT

CASE REPORT

Three years prior to presentation, a 50 year-old African American woman was diagnosed with sarcoidosis following the discovery of bilateral hilar adenopathy and biapical nodularity through contrast-enhanced computed tomography (Figures 11 and 12). The discovery was incidental, as she was having a CT of the chest, abdomen, and pelvis to follow-up a previously identified benign duodenal mass. Of note, the duodenal mass was not present on this follow-up exam. She was referred back to her outside general medical practitioner for workup, and while the medical records regarding this workup were unobtainable, it was confirmed that she indeed was diagnosed with sarcoidosis. Per her history, over the past three years she has developed clinical symptoms of pulmonary disease, for which she is being treated.

Six months prior to presentation, her medical doctor ordered a CT of her chest and abdomen to evaluate the status of her pulmonary disease, and to see if there had been any extrapulmonary manifestations (Figure 10). An abnormal, hypodense mass on the left renal superior pole was incidentally discovered, and she was referred to us for magnetic resonance to evaluate for the possibility of a carcinoma based on an outside interpretation of the CT. She denied any urinary symptoms, as well as any abdominal or flank pain. The MRI demonstrated a peripheral region of renal parenchymal tissue within the superior posterior cortex of the left kidney with abnormal signal (Figures 1-7). It measured 3.2 x1.5 cm. There was mild contrast enhancement on initial arterial phase imaging and subtraction imaging, however it demonstrated slower enhancement than the remainder of the renal cortex. The borders were ill-defined, extended into cortical margins, and there was no evidence of inflammatory change.

The initial differential diagnosis included lymphoma and infarction, but less likely carcinoma of the renal parenchyma. Upon further review of the imaging and an extensive review of literature, the possibility of pseudotumorous renal sarcoidosis was entertained, especially given her known history of sarcoidosis. Nevertheless, it was understood that such a

manifestation of sarcoidosis is extremely rare, and histologic evidence would be needed to rule out these other possibilities.

Biopsy of the mass was indicated, however it was delayed secondary to the patient's apprehension of the procedure. Two months following the MRI, the interventional radiology service performed a CT-guided biopsy of the renal mass (Figure 9). The cytology obtained from the fine needle aspirate demonstrated mixed lymphoid cells with rare multinucleate giant cells suggestive of granulomata. Microscopic examination of Hematoxylin and Eosin-stained histologic section (Figure 13 a-d) showed needle core biopsy fragments of renal cortical tissue, distorted by multiple non-necrotizing granulomata and chronic interstitial inflammation. The granulomata were composed of epithelioid histiocytes including multinucleated giant cells and surrounded by few small mature appearing lymphocytes. Few giant cells with concentric calcifications consistent with Schaumann bodies were present. Gomori-Grocott methenamine silver (GMS) and acid-fast bacteria (AFB) histochemical stains were negative for fungal organisms and mycobacteria, respectively. No areas of necrosis nor evidence of malignancy were identified. These findings were deemed compatible with sarcoidosis, in concordance with the patient's history.

Of note, laboratory measurements such as angiotensin converting enzyme and vitamin D were not obtained as their diagnostic value serves more for the initial diagnosis, and is not necessarily an accurate measurement of disease activity [1].

DISCUSSION

Sarcoidosis is an enigmatic disease, with environmental, genetic, and immunologic factors as suspected contributors to its pathologic development, but with no clearly defined cause [1]. Epidemiologically, the incidence of sarcoidosis among black Americans is nearly three times that of white Americans, and has been described as more likely to be chronic, less responsive to treatment, and fatal in this racial group [2]. Women are more likely than men to be afflicted, regardless of race or ethnicity. While low socioeconomic status does not increase the risk of sarcoidosis, financial barriers often result in more severe presentation at the time of diagnosis [3].

Sarcoidosis is still considered a diagnosis of exclusion, and generally requires clinical and radiographic evidence that is then corroborated by biopsy of affected organs for the identification of non-necrotizing granulomata. Histologic examination is also important to exclude other possible well-known causes of granulomatous inflammation, in particular infectious etiology [1]. While there are characteristic manifestations of the disease, clinical presentations vary from asymptomatic/incidental discovery to organ failure, and literature reports implicate practically every organ as a potential site for disease [2]. Pulmonary manifestations are present in greater than 90% of patients with sarcoidosis. Classic radiographic imaging of the chest, whether obtained to workup respiratory symptoms or discovered incidentally, may reveal bilateral hilar adenopathy and/or reticular parenchymal opacities [4]. High resolution CT of the chest may reveal a variety of additional abnormalities, including nodularity, bronchial wall thickening, and stranding with predominance in the middle and apical regions of the lungs [5]. Staging occurs through features seen on chest radiographs, however the prognostic value of such stages regarding respiratory function is uncertain [6].

The granulomata in sarcoidosis have similar morphologic features regardless of the organ affected. They are composed of tightly packed clusters of histiocytes, including epithelioid and giant multinucleated forms, surrounded by few lymphocytes (naked granuloma), mast cells and fibroblasts [7, 8]. They can be coalescent and usually follow lymphatic pattern of distribution and may show angioinvasion. Small amounts of necrosis may be present and do not exclude the diagnosis of sarcoidosis. A variety of cytoplasmic inclusions maybe present in the cytoplasm of giant cells including Schaumann (Conchoidal) bodies and birefringent calcium oxalate crystals (lamellated concentric calcifications, asteroid bodies (stellate inclusions with multiple rays radiating from central core), and Hamazaki-Wesenberg bodies (known as yellow/brown/spindle bodies and represent giant intracellular lysosomes, which can also be extracellular [8-12]. It is important to keep in mind that the granulomata and inclusions are nonspecific and not every nonnecrotizing granulomata of undetermined etiology is sarcoidosis. The rule of pathology is to exclude other well known causes of granulomatous inflammation using organism-specific histochemical stains or preferably by microbiologic cultures of fresh biopsy tissue.

Extrathoracic involvement in sarcoidosis is not uncommon, occurring in up to 30% of patients. The temporal relationship to pulmonary manifestations is unpredictable, as they may occur before, after, or coincidentally with the lung disease, and rarely there may only be extrapulmonary manifestations present [13]. Dermatologic and ocular manifestations are the most common extrapulmonary complications of sarcoidosis, however imaging studies are of limited use. Neurosarcoidosis is a relatively uncommon, yet well-documented phenomenon in which the brain, spinal cord, meninges, and cranial nerves may be involved. Diagnostic imaging, preferentially through contrast-enhanced MRI, is important in the workup and may allow avoidance of invasive biopsies, although the lesions are not specific for sarcoid [14]. Cardiac involvement, while usually not clinically apparent, has been seen often in post-mortem studies of patients with known sarcoidosis. Because the initial presentation of cardiac sarcoid can be a fatal arrhythmia, screening for cardiac involvement has been suggested [15]. Although an exact strategy is unknown, cardiac MR is proving to be valuable for the visualization of scar tissue and myocardial inflammation in non-ischemic distributions, allowing for either the empirical deduction of cardiac involvement, or the guidance of definitive biopsies [16]. Sarcoid manifestations in the liver and spleen are the most common intraabdominally, with clinical or radiographic diagnosis occurring between 20-25% of cases. Hepatomegaly and splenomegaly from granulomatous infiltration are more common, however hepatic and splenic nodules formed from coalescent granulomata are also potential presentations. The nodules, are multiple, well-defined,

hypoechogenic on ultrasound, and hypodense on CT. These nonspecific imaging findings are similar to those of malignant metastases and lymphoma, and tissue biopsy is necessary for differentiation [17].

Renal disease is a well-documented occurrence in the pathophysiology of sarcoidosis, but does not always indicate granulomatous infiltration into the renal parenchyma. The most common cause of chronic kidney disease from sarcoidosis is nephrocalcinosis secondary to granulomatous production of calcitriol resulting in hypercalcemia. These granulomata are typically extrarenal [18]. Rarely, direct granulomatous involvement of the kidneys is observed but typically does not impair renal function. Radiologic studies are therefore often necessary to detect direct granulomatous involvement in patients with suggestive clinical history. Interstitial nephritis is a possible manifestation, and may demonstrate a striated nephrogram on contrast-enhanced CT [19]. Glomerular nephritis from direct infiltration may also occur.

Granulomatous pseudotumors, as was the presentation in this case report, are exceedingly rare presentations of renal sarcoidosis. Only a few pathology-proven case reports have described such manifestations [20,21]. The case reported by Lockhart et al described the patient as having hematuria and back pain, whereas the case reported by Heldman et al reported the mass as incidentally found, as was the situation in this case report, following a CT to evaluate hilar adenopathy. These pseudotumors may be singular or multiple, unilateral or bilateral. They may be echogenic on ultrasound [22]. They are focal, exophytic nodules that may exhibit hypo-, iso-, or hyperdense attenuation on noncontrast CT relative to the normal renal parenchyma, but are hypo-enhancing on contrast-enhanced CT [20-22]. On MRI, reported cases as well as this case demonstrate poor circumscription of the mass or masses from the renal parenchyma, indicating interstitial infiltration. On unenhanced T1 and T2-weighted imaging, the pseudotumor may be homogenous or slightly heterogenous, predominately remaining isointense to the surrounding renal parenchyma [20-22]. Following gadolinium-based intravenous contrast, there is less early and delayed enhancement relative to the normal renal cortex on both T1 and T2 imaging, a consistent feature reported in all available case reports that have evaluated these masses by MRI. Whole-body positron emission tomography (PET) using 18F-fluorodeoxyglucose (18F-FDG) has been performed and demonstrated intense radiotracer uptake by such masses, which limits its value because of the inability to differentiate such masses from malignancies. The differential diagnosis for a hypoenhancing, infiltrative renal mass is extensive, and includes renal parenchymal carcinomas, locally invasive transitional cell carcinomas, metastases, lymphomas, infection (xanthogranulomatous pyelonephritis), angiomyolipomas, oncocytoma or other inflammatory processes (Table 2) [23-28]. However, while the radiographic findings of pseudotumorous renal sarcoid are difficult to differentiate from these other potential, and often more likely diagnoses, the clinical history, laboratory data, and/or presence of classical features of sarcoidosis may support entertaining it as a possible diagnosis, which may dramatically alter clinical management. Entertaining such a diagnosis, under the correct clinical scenario, is important because the alternative diagnoses, particularly genitourinary malignancies, require tissue sampling for diagnosis, and nondiagnostic core-needle biopsy may prompt more invasive surgical intervention for diagnosis [29].

Treatment of pseudotumoral renal sarcoidosis may be deferred unless symptoms develop, principally obstructive uropathy or renal interstitial disease, both of which may manifest as renal insufficiency, and differentiated with imaging [1]. The mainstay treatment of symptomatic pseudotumoral renal sarcoidosis is no different than the pulmonary or other extrapulmonary manifestations of sarcoidosis, with first line therapy consisting of high-dose, long-term corticosteroids, with trials of other renal-sparing immunosuppresants if corticosteroids are ineffective [13,18]. Additionally, standard renal-protective measures such as strict blood pressure and glucose control, and ACE-inhibition should be implemented, as well as relief of mechanical obstruction, if present.

TEACHING POINT

Sarcoidosis is a disease of unclear etiology characterized by non-caseating granulomatous infiltrates, classically found in the lungs, but commonly found in other organs as well. Pseudotumorous granulomatous renal masses are an exceedingly rare, albeit documented manifestation of sarcoidosis, and should be considered in the differential of infiltrative renal parenchymal masses, especially in a patient with a history of sarcoid, as such a diagnosis can drastically alter clinical management.

REFERENCES

1. Iannuzzi MC, Rybicki BA, Teirstein AS. Sarcoidosis. N Engl J Med. 2007;357(21):2153-2165. PMID: 18032765

2. Baughman RP, Teirstein AS, Judson MA, Rossman MD, Yeager H Jr, Bresnitz EA, DePalo L, Hunninghake G, Iannuzzi MC, Johns CJ, McLennan G, Moller DR, Newman LS, Rabin DL, Rose C, Rybicki B, Weinberger SE, Terrin ML, Knatterud GL, Cherniak R. Clinical characteristics of patients in a case control study of sarcoidosis. Am J Respir Crit Care Med 2001;164:1885-1889. PMID: 11734441

3. Rabin DL, Thompson B, Brown KM, Judson MA, Huang X, Lackland DT, Knatterud GL, Yeager H Jr, Rose C, Steimel J. Sarcoidosis: social predictors of severity at presentation. Eur Respir J 2004;24:601-608. PMID: 15459139

4. Baughman RP. Pulmonary sarcoidosis. Clin Chest Med. 2004;25(3):521-530. PMID: 15331189

5. Müller NL, Mawson JB, Mathieson JR, Abboud R, Ostrow DN, Champion P. Sarcoidosis: correlation of extent of

disease at CT with clinical, functional, and radiographic findings. Radiology. 1989;171(3):613-618. PMID: 2717730

6. Nunes H, Uzunhan Y, Gille T, Lamberto C, Valeyre D, Brillet PY. Imaging of sarcoidosis of the airways and lung parenchyma with correlation with lung function. Eur Respir J. 2012. [Epub ahead of print] doi: 10.1183/09031936.00025212. PMID: 22790910

7. Adams DO. The biology of the granuloma. In: Ioachim HL, eds. Pathology of Granulomas. New York: Raven; 1983:1-20

8. Jones Williams W. The nature and origin of Schaumann bodies. J Pathol Bacteriol 1960;79:193-201. PMID: 13853169

9. Reid JD, Andersen ME. Calcium oxalate in sarcoid granulomas. Am J Clin Pathol 1988;90:545-558

10. Rosen Y, Vuletin JC, Pertschuk LP, Silverstein E. Sarcoidosis from the pathologist's vantage point. Pathol Annu 1979;14(Part 1):405-439. PMID: 229453

11. Hamazaki T. Uber ein neues, sauerfeste Substanz fuhrendes Spindelkorperchen der Menschlichen Lymphdru¨sen. Virchows Arch A Pathol Pathol Anat 1938;301:490-522

12. Wesenberg W. On acid-fast Hamazaki spindle bodies in sarcoidosis of lymph nodes and on double refractile cell inclusions in sarcoidosis of the lungs. Arch Klin Exp Dermatol 1966;227:101-107. PMID: 5984747

13. Rizzato G, Palmieri G, Agrati AM, Zanussi C. The organ-specific extrapulmonary presentation of sarcoidosis: a frequent occurrence but a challenge to an early diagnosis. A 3-year-long prospective observational study. Sarcoidosis Vasc Diffuse Lung Dis. 2004;21(2):119-126. PMID: 15281433

14. Burns TM. Neurosarcoidosis. Arch Neurol. 2003; 60; 1166-1168. PMID: 12925378

15. Kim JS, Judson MA, Donnino R, Gold M, Cooper LT, Prystowsky EN, and Prystowsky S. Cardiac sarcoidosis. Amer Heart J.2009; 157(1): 9-21. PMID: 19081391

16. Vignaux O, Dhote R, Duboc D, Blanche P, Devaux JY, Weber S, Legmann P. Detection of myocardial involvement in patients with sarcoidosis applying T2-weighted, contrast-enhanced, and cine magnetic resonance imaging: initial results of a prospective study. J Comput Assist Tomogr. 2002; 26:762-767. PMID: 12439312

17. Kahi CJ, Saxena R, Temkit M, Canlas K, Roberts S, Knox K, Wilkes D, Kwo PY. Hepatobiliary disease in sarcoidosis. Sarcoidosis Vasc Diffuse Lung Dis. 2006; 23:117-123. PMID: 17937107

18. Muther RS, McCarron DA, Bennett WM. Renal manifestations of sarcoidosis. Arch Intern Med. 1981;141(5):643-645. PMID: 7224744

19. Koyama T, Ueda H, Togashi K, Umeoka S, Kataoka M, Nagai S. Radiologic Manifestations of Sarcoidosis in Various Organs. Radiographics. 2004; 24:87-104. PMID: 14730039

20. Lockhart ME, Smith JK, Kenney PJ, Urban DA. Pseudotumorous renal involvement of sarcoidosis J Urol. 2001; 165: 895. PMID: 11176498

21. Heldmann M, Behm W, Reddy MP, Bozeman C, Welman G, Abreo F, Minagar A. Pseudotumoral renal sarcoid: MRI, PET, and MDCT appearance with pathologic correlation. AJR Am J Roentgenol. 2005; 185: 697-699. PMID: 16120920

22. Herman TE, Shackelford GD, McAlister WH. Pseudotumoral sarcoid granulomatous nephritis in a child: case presentation with sonographic and CT findings. Pediatr Radiol. 1997 Sep;27(9):752-4. PMID: 9285739

23. Thompson RH, Kurta JM, Kaag M, Tickoo SK, Kundu S, Katz D, Nogueira L, Reuter VE, Russo P. Tumor size is associated with malignant potential in renal cell carcinoma cases. J Urol. 2009;181(5):2033. PMID: 19286217

24. Israel GM, Bosniak MA. An update of the Bosniak renal cyst classification system. Urology. 2005;66(3):484. PMID: 16140062

25. Siegel CL, Middleton WD, Teefey SA, McClennan BL. Angiomyolipoma and renal cell carcinoma: US differentiation. Radiology. 1996;198(3):789-93. PMID: 8628873

26. Verswijvel G, Oyen R, Van Poppel H, Roskams T. Xanthogranulomatous pyelonephritis: MRI findings in the diffuse and the focal type. Eur Radiol. 2000;10(4):586-9. PMID: 10795538

27. Prasad SR, Surabhi VR, Menias CO, Raut AA, Chintapalli KN. Benign renal neoplasms in adults: cross-sectional imaging findings. AJR Am J Roentgenol. 2008;190(1):158-64. PMID: 18094306

28. Vikram R, Sandler CM, Ng CS. Imaging and staging of transitional cell carcinoma: part 2, upper urinary tract. AJR Am J Roentgenol. 2009;192(6):1488-93. PMID: 19457809

29. Volpe A, Kachura JR, Geddie WR, Evans AJ, Gharajeh A, Saravanan A, Jewett MA. Techniques, safety and accuracy of sampling of renal tumors by fine needle aspiration and core biopsy.
J Urol. 2007. 178(2):379-86. PMID: 17561170

FIGURES

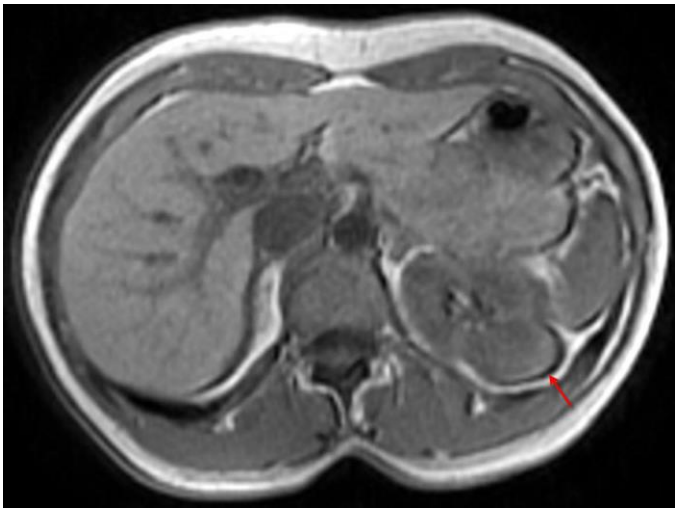

Figure 1: 53 year old female with biopsy proven renal sarcoid. Noncontrast T1 image demonstrates an ill defined exophitic left renal mass (red arrow), with isointense to mildly hyperintense signal within the lesion. (GE Signa HDx 1.5T T1 weighted noncontrast axial sequence, TR 150, TE 1)

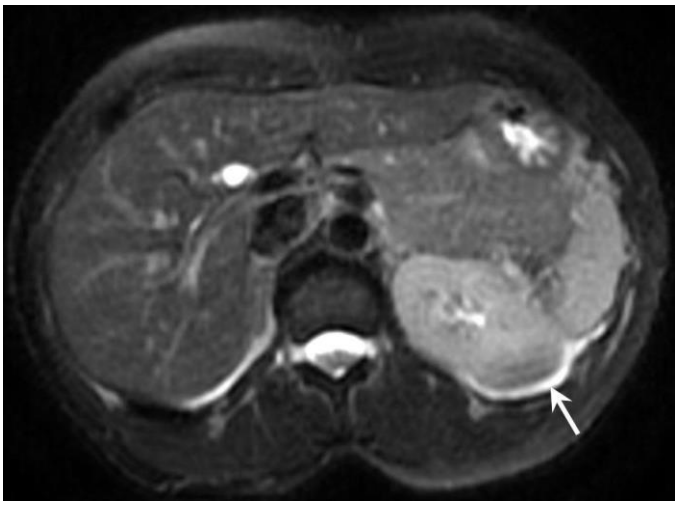

Figure 2: 53 year old female with biopsy proven renal sarcoid. Noncontrast T2 image demonstrates an ill defined exophitic left renal mass (white arrow), with isointense to slightly hyperintense signal within the lesion. (GE Signa HDx 1.5T T2 weighted noncontrast fat saturated axial sequence, TR 2000, TE 87)

Figure 3: 53 year old female with biopsy proven renal sarcoid. Arterial phase postcontrast T1 image demonstrates an ill defined exophitic left renal mass (white arrow), with minimal early enhancement. (GE Signa HDx 1.5T T1 weighted LAVA fat saturated axial sequence, TR 4, TE 2, Arterial postcontrast 12cc Omniscan injection)

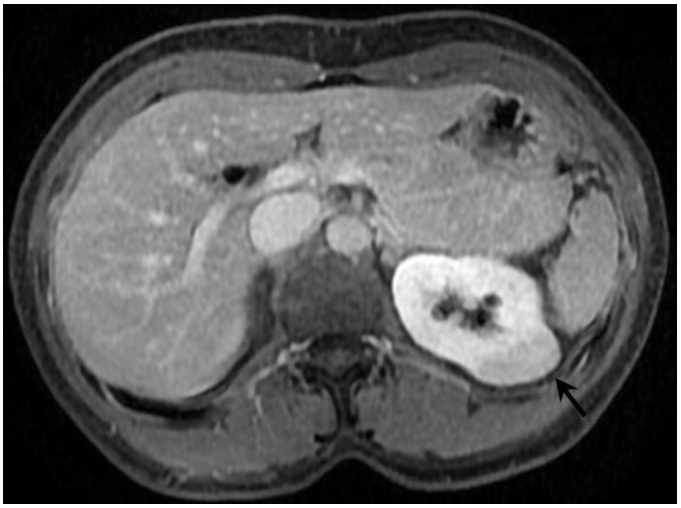

Figure 4: 53 year old female with biopsy proven renal sarcoid. Venous phase postcontrast T1 image demonstrates an ill defined exophitic left renal mass (black arrow), with delayed enhancement to a lesser degree than the surrounding normal renal parenchyma. (GE Signa HDx 1.5T T1 weighted LAVA fat saturated axial sequence, TR 4, TE 2, Venous postcontrast 12cc Omniscan injection)

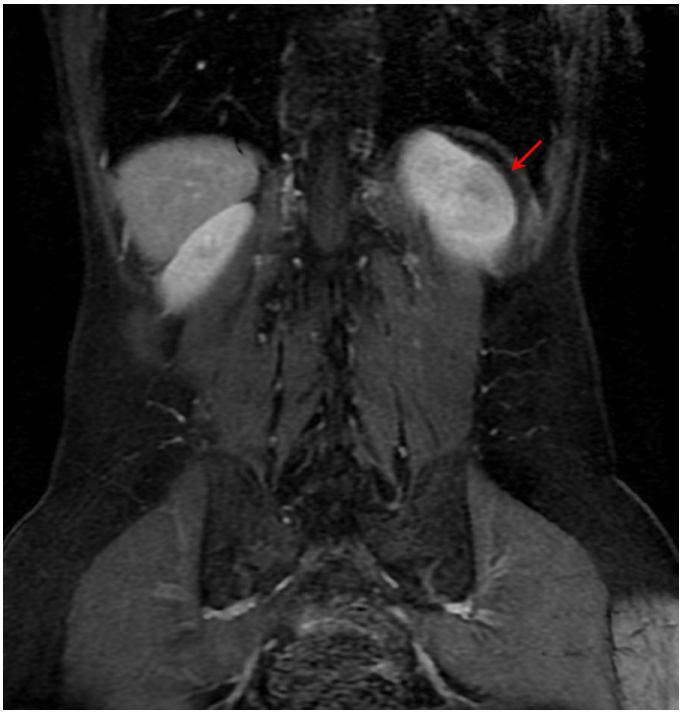

Figure 5: 53 year old female with biopsy proven renal sarcoid. Venous phase postcontrast T1 image demonstrates an ill defined exophitic left renal mass (red arrow), with delayed enhancement to a lesser degree than the surrounding normal renal parenchyma. Due to the only partially exophitic nature of the lesion and subtle signal differentiation, the lesion was much less evident in the coronal plane as compared to the axial plane on all coronal sequences, including CT reconstructions. (GE Signa HDx 1.5T T1 weighted LAVA fat saturated coronal sequence, TR 4, TE 2, Venous postcontrast 12cc Omniscan injection)

Figure 6: 53 year old female with biopsy proven renal sarcoid. Arterial phase postcontrast T1 image demonstrates an ill defined exophitic left renal mass (white arrow), with minimal early enhancement. (Siemens Avanto 1.5T T1 weighted VIBE fat saturated axial sequence, TR 5, TE 2, Arterial postcontrast 12cc Omniscan injection)

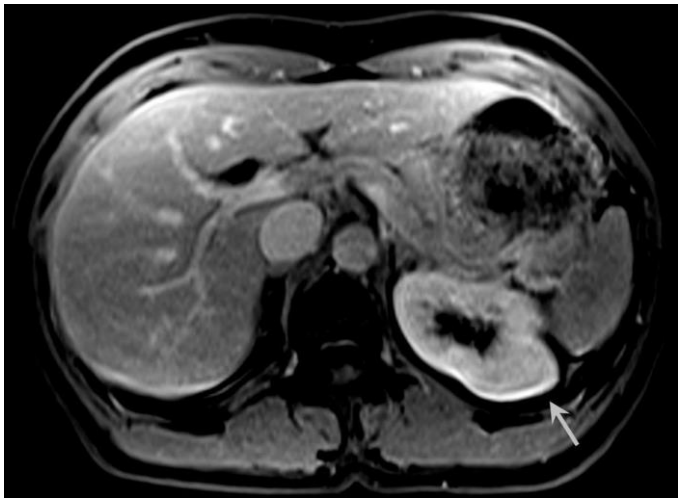

Figure 7: 53 year old female with biopsy proven renal sarcoid. Venous phase postcontrast T1 image demonstrates an ill defined exophitic left renal mass (white arrow), with delayed enhancement to a slightly lesser degree than the surrounding normal renal parenchyma. (Siemens Avanto 1.5T T1 weighted VIBE fat saturated axial sequence, TR 5, TE 2, Venous postcontrast 12cc Omniscan injection)

Figure 8: 53 year old female with biopsy proven renal sarcoid. Subtracted postcontrast T1 image demonstrates an ill defined exophitic left renal mass (white arrow), with mild enhancement to a lesser degree than the surrounding normal renal parenchyma. (GE Signa HDx 1.5T T1 weighted LAVA fat saturated axial sequence, TR 4, TE 2, Venous-arterial postcontrast subtraction 12cc Omniscan injection)

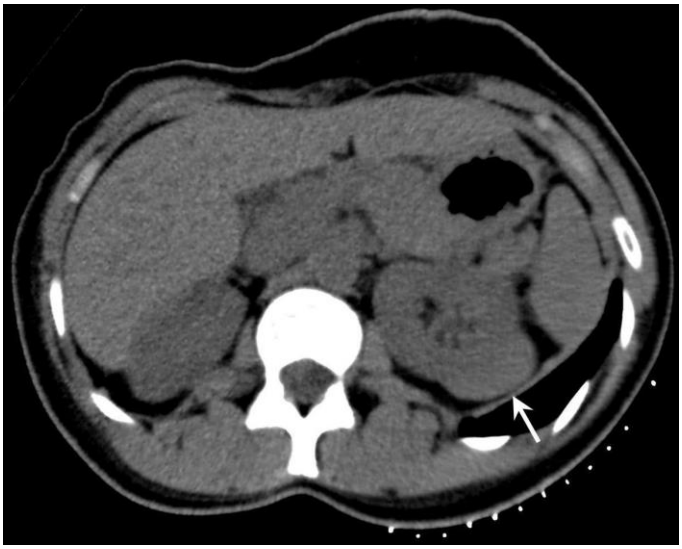

Figure 9: 53 year old female with biopsy proven renal sarcoid. Noncontrasted CT prior to biopsy demonstrates an ill defined exophitic left renal mass (white arrow), with slightly hyperdense attenuation within the lesion. (Toshiba Aquilion 320-slice CT, noncontrasted, 5mm slice thickness, kVp 120)

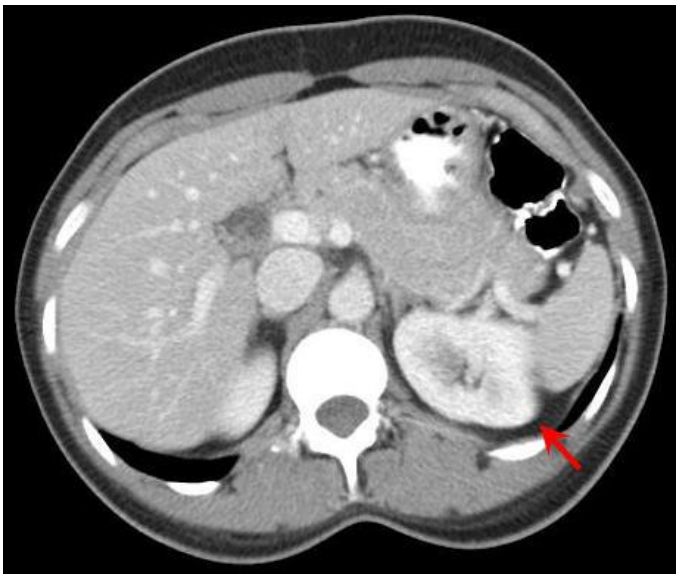

Figure 10: 53 year old female with biopsy proven renal sarcoid. Contrasted CT axial image demonstrates an ill defined cortical left renal mass (red arrow), with enhancement features similar to that of the normal kidney, but around an encapsulated lesion. CT examination of the chest and abdomen with intravenous contrast (Omnipaque 300). (CT scanner: LightSpeed 16; Mag: 1.7x; 120 kV; 100-300 mA; 5.0 mm Tilt: 0.0; ET: 0.8 s; GP: 0.6 s; TS: 17.50 mm/s; W: 400. L: 40; 512 x 512 Matrix; DFOV: 34.5 x 34.5 cm)

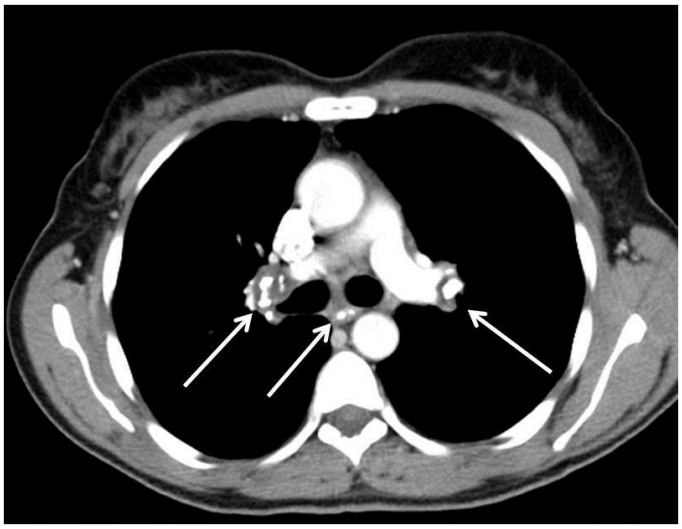

Figure 11: 53 year old female with an calcified mediastinal and hilar lymphadenopathy, known to be secondary to sarcoidosis. Contrasted axial CT images (soft tissue windows) demonstrate the calcified subcarinal and bilateral hilar lymph nodes. . CT examination of the chest and abdomen with intravenous contrast (Omnipaque 300). (CT scanner: LightSpeed 16; Mag: 1.7x; 120 kV; 100-300 mA; 5.0 mm Tilt: 0.0; ET: 0.8 s; GP: 0.6 s; TS: 17.50 mm/s; W: 400. L: 40; 512 x 512 Matrix; DFOV: 34.5 x 34.5 cm)

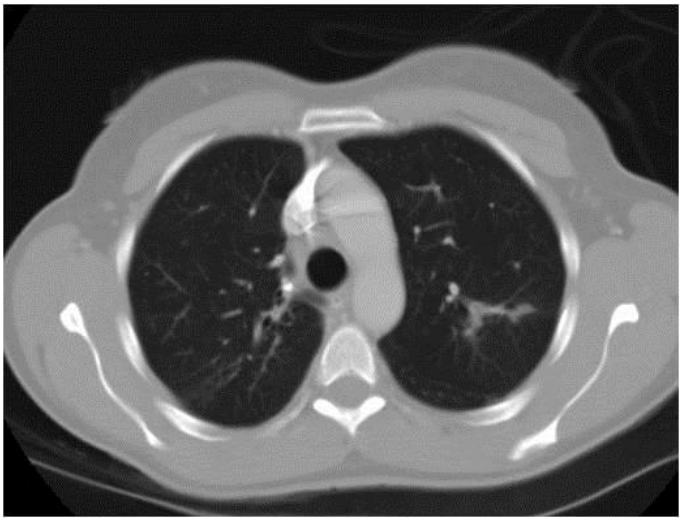

Figure 12: 53 year old female with a known history of sarcoidosis. Contrasted axial CT images (lung windows) demonstrate peribronchovascular nodularity. CT examination of the chest and abdomen with intravenous contrast (Omnipaque 300). (CT scanner: LightSpeed 16; Mag: 1.7x; 120 kV; 100-300 mA; 5.0 mm Tilt: 0.0; ET: 0.8 s; GP: 0.6 s; TS: 17.50 mm/s; W: 400. L: 40; 512 x 512 Matrix; DFOV: 34.5 x 34.5 cm)

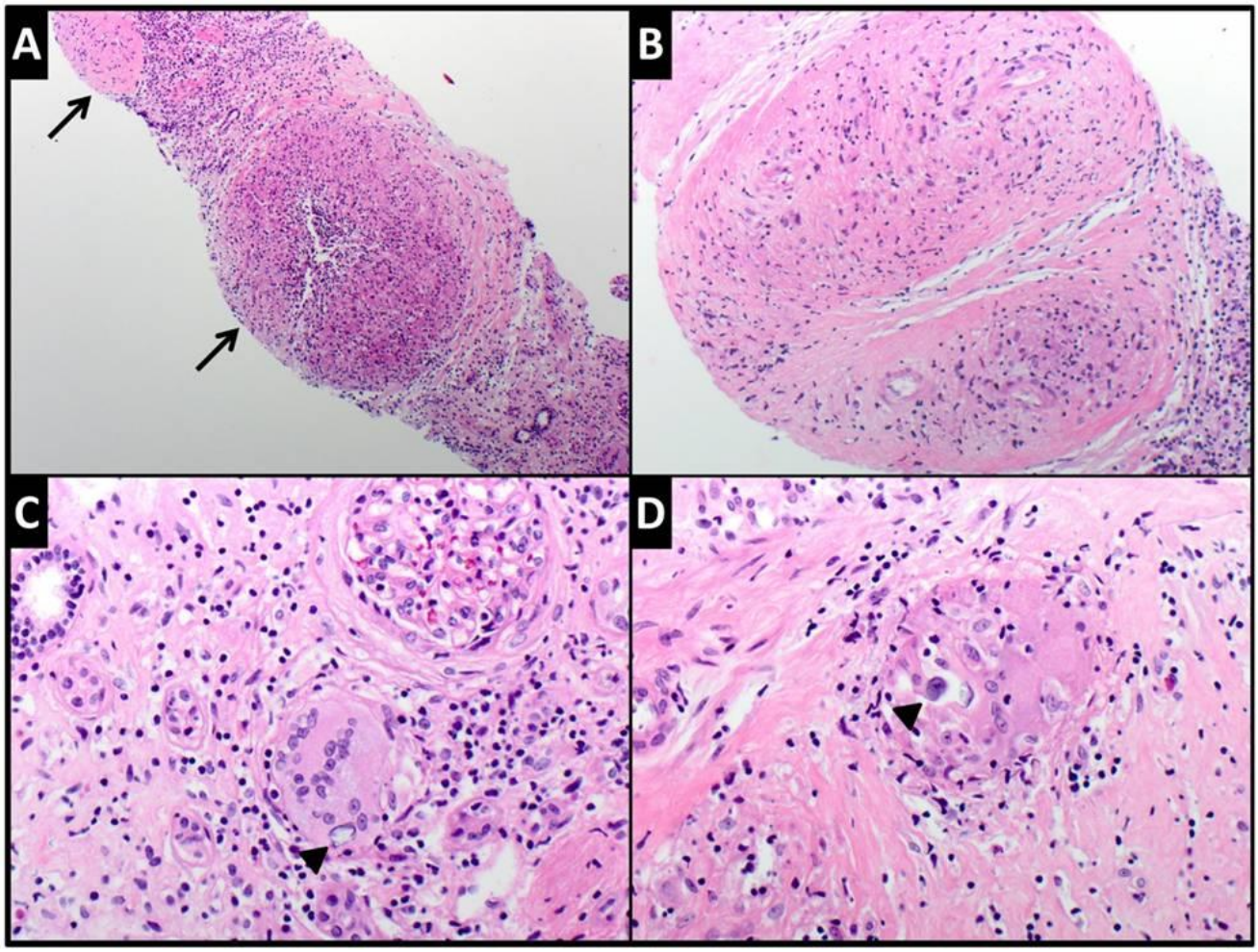

Figure 13: Composite photomicrograph showing the microscopic findings in the renal biopsy from this case. Low (A) and intermediate (B) power views showing multiple nonnecrotizing granulomata (arrows) in renal parenchyma. They are composed of epithelioid histiocytes, including some giant forms. Giant cells with concentric calcifications consistent with Schaumann bodies (arrow heads) are shown in C and D (Hematoxylin and eosin stained-sections, original magnifications X40, X100, X200 and X400 respectively).

Etiology	• Exact etiology remains elusive
	• Likely multifactorial
	  o Environmental exposure
	  o Infectious agents
	  o Immunogenetic
	  ▪ Major histocompatibility complexes
	  ▪ T-cell abnormalities
	  ▪ T-cell receptor reactivitiy [1]
	• Renal involvement either due to hypercalcemia/hypercalcuria from increased calcitriol production, or from direct granulomatous infiltration.
	• Underlying etiology remains the same for all organs [18].

Incidence	• In the United States, the incidence of any form of sarcoidosis among black Americans is about 35.5 cases per 100,000, which is about three times that of white Americans, which is 10.9 per 100,000. [1] • Incidence of renal involvement in sarcoidosis is unknown. There have been less than ten case reports of pseudotumorous granulomatous infiltration of the kidneys [18-22].
Gender Ratio	• Predilection for females developing any form of sarcoidosis • Variable gender ratio, tends to be around 2:1 females to males [1]. • Uncertain if there is a specific gender predilection for renal involvement in sarcoidosis [18].
Age Predilection	• Black Americans: the peak incidence of sarcoidosis is in the fourth decade for both men and women. • Other ethnic and racial groups, the age of onset is variable. • All cases considered, the majority present between the ages of 10 and 40. • Young children and the elderly may still present with the disease, likely will be atypical presentation [1-3].

Risk Factors	• The lifetime risk of sarcoidosis is in black Americans at 2.4%
	  o Black Americans tend to develop more acute, severe disease
	• That of white Americans at 0.85%.
	  o Whites may be asymptomatic or have mild, chronic disease.
	• Associations with specific immune-related genes (HLA DR 11, 12, 14, 15, and 17) have been made and seem to confer increased susceptibility.
	• Exposure to hazardous occupational and environmental particulates has been hypothesized to increase the risk.
	  o Specific exposures are unknown.
	• People of a lower socioeconomic are more likely to present at more advanced stages because of lack of access to healthcare [1-4].

Treatment	• First line treatment for both pulmonary and extrapulmonary manifestations in symptomatic patients is prolonged glucocorticoid therapy
	• Dosing is dependent on the severity of the symptoms and the rate at which they are progressing
	  o Usually is initiated at 20-40mg of prednisone daily for moderately severe symptoms
	  o 80-100mg daily for severe respiratory, cardiac, neurologic, or ocular disease.
	• Initial therapy lasts for 4-12 weeks depending on response,
	• Maintenance therapy at about half the dose continues for 6-12 months
	• Response to therapy is monitored based on functional status as well as comparative imaging, although there is no standardized way to monitor therapy
	• Methotrexate, azathioprine, leflunomide, and antimalarials are all possible alternatives to those not responding to or intolerant of glucocorticoids [1,4].

Prognosis	• The overall mortality from sarcoidosis is less than 5%
	  o Stems from pulmonary fibrosis, pulmonary hemorrhage, or arrhythmia secondary to myocardial involvement.
	• Patients who are responsive to treatment and are relapse-free after a year are unlikely to have relapses.
	• Relapses may occur during tapering of therapy or within the first year following cessation of therapy, and chronic low-dose steroid therapy may be necessary [1].
	• In renal sarcoidosis, if the kidney function has been affected by the fibrosis and inflammation, there is less probability of regaining full kidney function.
	  o If kidney involvement is extensive, a patient may need dialysis or a transplant [18].

Table 1: Summary table for sarcoidosis (continued on next page)

Findings on Imaging	• Lungs:
	  ○ Classic radiographic imaging of the chest, may reveal
	  ▪ bilateral hilar adenopathy
	  ▪ reticular parenchymal opacities [4].
	  ○ High resolution CT of the chest may reveal
	  ▪ nodularity
	  ▪ bronchial wall thickening
	  ▪ stranding
	  ▪ predominance in the middle and apical regions of the lungs
	• Heart:
	  ○ Cardiac MR is valuable for the visualization of
	  ▪ scar tissue
	  ▪ myocardial inflammation in non-ischemic distributions [15, 16].
	• Liver and Spleen:
	  ○ Sarcoid manifestations in the liver and spleen are the most common intraabdominally
	  ○ Hepatomegaly and splenomegaly from granulomatous infiltration
	  ○ Hepatic and splenic nodules formed from coalescent granulomata are also potential presentations.
	  ▪ The nodules are multiple, well-defined, hypoechogenic on ultrasound, and hypodense on CT [17].
	• Kidneys:
	  ○ Interstitial nephritis is a possible manifestation
	  ▪ May demonstrate a striated nephrogram on contrast-enhanced CT [18, 19]
	  ○ Renal Pseudotumors:
	  ○ May be singular or multiple
	  ○ Unilateral or bilateral.
	  ○ They may be echogenic on ultrasound [22].
	  ○ Focal, exophytic nodules that may exhibit hypo-, iso-, or hyperdense attenuation on noncontrast CT relative to the normal renal parenchyma, but are hypo-enhancing on contrast-enhanced CT [20-22].
	  ○ MRI,
	  ▪ Poor circumscription of the mass or masses from the renal parenchyma, indicating interstitial infiltration.
	  ▪ On unenhanced T1 and T2-weighted imaging, the pseudotumor may be homogenous or slightly heterogeneous, predominately remaining isointense to the surrounding renal parenchyma [20-22].
	  ▪ Following gadolinium-based intravenous contrast, there is less early and delayed enhancement relative to the normal renal cortex on both T1 and T2 imaging, a consistent feature reported in all available case reports that have evaluated these masses by MRI.
	  ○ Whole-body PET using ^{18}F-FDG has demonstrated intense radiotracer uptake by such masses.

Table 1: Summary table for sarcoidosis (continued)

Pathology	X-ray	US	CT	MRI	PET
Renal Sarcoid	Very limited unless mass is large enough to distort renal contour	Both hypo- and hyperechoic masses have been reported; well-defined, exophytic [21, 22]	Focal, exophytic nodules that may exhibit hypo-, iso-, or hyperdense attenuation on noncontrast CT relative to the normal renal parenchyma; poorly enhancing on all phases of contrast-enhanced CT. Typically well-differentiated from functional kidney [20-22]	On unenhanced T1 and T2-weighted imaging, the pseudotumor may be homogenous or slightly heterogonous, predominately remaining isointense to the surrounding renal parenchyma Less early and delayed enhancement relative to the normal renal cortex on both T1 and T2 imaging. [21]	One report described intense radiotracer uptake [21]
Renal Cell Carcinoma	Very limited unless there are calcifications or mass is large enough to distort renal contour	More value if tumor is larger. Can be hypo-, iso-, or hyperechoic, and heterogeneous. Most likely followed by CT [23, 25]	Dedicated renal CT with noncontrast, corticomedullary, nephrographic, and excretory phase. May demonstrate hypo-, iso-, or hyperattenuation relative to renal parenchyma on noncontrast CT. Best seen on nephrographic phase, is heterogeneous, hypoattenuating vascular mass relative to homogenously enhancing renal parenchyma [23, 25]	Iso or hypo-intense on T1 relative to normal kidney. Clear cell carcinoma may show loss of signal intensity with chemical shift imaging. Hyperintense and heterogonous on T2. [23, 25, 27]	Demonstrate increased FDG uptake.
Transitional Cell Carcinoma	May see large renal outline in obstructed kidney. May see calcifications on tumor surface. IV urography may demonstrate filling defects in collecting system. Overall, limited usefulness [28]	Hypoechoic mass in the renal collecting system. Evidence of hydronephrosis. Focal hypoechogenic mass extending into renal cortex may indicate local invasion [28].	Filling defects of collecting system, obstruction and dilatation proximal to lesion. Hypo- or iso-attenuated relative to renal parenchyma, hyperattenuated relative to urine on noncontrast CT. On excretory phase show mild to moderate enhancement, less so than urine [28].		
Oncocytoma	Very limited unless there are calcifications or mass is large enough to distort renal contour, both of which are rare [27]	Well-defined, homogenous, hypo- to isoechoic. Cannot always see central scar, but may be echogenic if large. Color Doppler may demonstrate radiating vessels [27]	Iso- to mildly hyperattenuating on noncontrast CT. Well-defined mass that is less attenuating on nephrographic phase relative to homogenously enhancing renal parenchyma. May show central hypoattenuating stellate scar. Can look exactly like RCC [27]	T1- well-defined, homogenous, iso- or hypointense relative to renal cortex T2- iso- or hypointense. Tumor scar may be hypointense on T1 and T2. Show homogenous enhancement with nonenhancing central scar after contrast [27].	Usually have less FDG uptake than RCC. Are typically isointense relative to renal parenchyma [27].

Table 2: Differential diagnosis table for renal sarcoidosis (continued on next page)

Pathology	X-ray	US	CT	MRI	PET
Lymphoma	Very limited unless mass is large enough to distort renal contour	Single or multiple homogenous, hypoechoic masses. May appear normal if small. May cause hydronephrosis.	Poorly enhancing, homogenous masses invading into renal parenchyma. Often present as multiple lesions, often bilateral. May cause bilateral renal enlargement, but doesn't necessarily disrupt renal contour. If necrotic, may become heterogonous or low density and mimic complicated cyst	Same diagnostic value as CT. Low intensity on T1. Iso- or moderately hyperintense on T2. Minimal enhancement, enhances to lesser degree than normal renal parenchyma	18F-FDG PET has high specificity for lymphoma, but not absolute. Nonpathologic accumulation of FDG occurs, but can often be identified as such
Xanthogranulomatous Pyelonephritis	Plain film may show renal stones or staghorn calculus. IV pyelography may show enlarged kidney or space-occupying lesion [26]	Enlarged kidney with loss of corticomedullary differentiation. Multiple hypoechoic masses [26]	Replacement of renal tissue by hypoattenuated areas with enhancing rims. May demonstrate fistula formation to perirenal organs. Clearly demonstrates renal stones [26].	Variable imaging presentation depending on fat content of mass. Can be hyperintense on T1 if high fat or hypointense if more focal and cystic. Chemical shift imaging may be valuable to observe fat content. Enhancement of cyst septa or heterogeneous enhancement may occur, or may not enhance depending on fat content [26]	May have high radiotracer uptake [26]
Angiomyolipoma	Plain film may demonstrate radiolucency if large quantity of fat is present. IV pyelogram may demonstrate distortion of collecting system. Low sensitivity and value [25].	Intense echogenicity with possibly shadowing. Usually well-circumscribed. Is not diagnostic of angiomyolipoma [25, 27].	Cortical, heterogeneous lesion with predominately fatty (low) attenuation. Variable enhancement pattern due to variety of components [25, 27].	High intensity on non-enhanced T1 because of fat content. Isointense to perinephric fat on T2. Fat-suppression is most sensitive for defining intratumoral fat [25, 27]	

Table 2: Differential diagnosis table for renal sarcoidosis (continued)

ABBREVIATIONS

18F-FDG = 18F-fluorodeoxyglucose
ACE = Angiotensin-converting enzyme
AFB = acid-fast bacteria (stain)
CT = Computed Tomography
GMS = Grocott methenamine silver (stain)
MRI= Magnetic Resonance Imaging
PET= Positron Emission Tomography

KEYWORDS

Sarcoidosis; Renal Sarcoidosis; Renal Mass; Pseudotumor

Online access

This publication is online available at:
www.radiologycases.com/index.php/radiologycases/article/view/1316

Peer discussion

Discuss this manuscript in our protected discussion forum at:
www.radiolopolis.com/forums/JRCR

Interactivity

This publication is available as an interactive article with scroll, window/level, magnify and more features.
Available online at www.RadiologyCases.com

Published by EduRad
www.EduRad.org